Video Article

A Multi-well Format Polyacrylamide-based Assay for Studying the Effect of Extracellular Matrix Stiffness on the Bacterial Infection of Adherent Cells

Effie E Bastounis[1], Fabian E Ortega[1], Ricardo Serrano[2], Julie A Theriot[3]

[1]Department of Biochemistry, Stanford University School of Medicine

[2]Department of Mechanical and Aerospace Engineering, University of California San Diego

[3]Departments of Biochemistry, Microbiology and Immunology and Howard Hughes Medical Institute, Stanford University School of Medicine

Correspondence to: Effie E Bastounis at ebastoun@stanford.edu

Abstract

Extracellular matrix stiffness comprises one of the multiple environmental mechanical stimuli that are well known to influence cellular behavior, function, and fate in general. Although increasingly more adherent cell types' responses to matrix stiffness have been characterized, how adherent cells' susceptibility to bacterial infection depends on matrix stiffness is largely unknown, as is the effect of bacterial infection on the biomechanics of host cells. We hypothesize that the susceptibility of host endothelial cells to a bacterial infection depends on the stiffness of the matrix on which these cells reside, and that the infection of the host cells with bacteria will change their biomechanics. To test these two hypotheses, endothelial cells were used as model hosts and *Listeria monocytogenes* as a model pathogen. By developing a novel multi-well format assay, we show that the effect of matrix stiffness on infection of endothelial cells by *L. monocytogenes* can be quantitatively assessed through flow cytometry and immunostaining followed by microscopy. In addition, using traction force microscopy, the effect of *L. monocytogenes* infection on host endothelial cell biomechanics can be studied. The proposed method allows for the analysis of the effect of tissue-relevant mechanics on bacterial infection of adherent cells, which is a critical step towards understanding the biomechanical interactions between cells, their extracellular matrix, and pathogenic bacteria. This method is also applicable to a wide variety of other types of studies on cell biomechanics and response to substrate stiffness where it is important to be able to perform many replicates in parallel in each experiment.

Video Link

The video component of this article can be found at https://www.jove.com/video/57361/

Introduction

Cells in most animal tissues are typically adherent, attaching both to neighboring cells and to their extracellular matrix (ECM). The anchorage of cells to their ECM is critical for many cellular processes ranging from cell motility to cell proliferation and survival[1,2]. Cellular anchorage to the ECM depends on both the ECM composition and stiffness. Cells respond to changes in the latter by dynamically re-arranging their cytoskeleton, cell-ECM and cell-cell adhesions, which in turn critically alter cell biomechanics and functions[3,4,5,6]. ECM stiffness can vary in space (*i.e.*, anatomic location), in time (*i.e.*, aging), and in pathophysiological processes (*e.g.*, arteriosclerosis, cancer, infections, *etc.*). For instance, it is widely accepted that endothelial cells residing on stiffer-as compared to softer-matrices exert increased forces to their ECM and to each other and exhibit increased motility and proliferation[7,8]. Likewise, fibroblasts residing on stiffer matrices impart high contractile forces to their ECM and show increased proliferation, motility, and ECM production[9,10,11]. Although cell mechanics and response to ECM stiffness have been studied extensively for various cell types, the relationship between adherent host cells, the stiffness of their ECM, and bacterial infections is still largely unknown.

To study the role of ECM stiffness in bacteria-host cell interactions, *L. monocytogenes* (Lm) was chosen as the model pathogen. Lm is a ubiquitous food-borne bacterium that can cause systemic infection in a wide variety of mammalian hosts. This facultative intracellular pathogen can move from the intestinal epithelium to distant organs by traversing different types of vascular endothelia. If it breaches the blood-brain barrier, Lm can cause meningitis, and when it crosses the placenta, it can cause spontaneous abortion[12,13]. Lm can infect different host cell types and can do so by using distinct pathogenic strategies. Lm infection has been studied mostly in the context of epithelial cells, while much less is known about how Lm can infect and bypass endothelial cells lining the lumen of blood vessels[14,15,16]. Moreover, it is still largely unknown how the stiffness of the ECM where endothelial cells reside modulates Lm's ability to invade these host cells and to then spread. Lm and several additional bacterial species (*i.e.*, *Rickettsia parkeri*) take advantage of the actin cytoskeleton of the host cells they infect to both invade into their cytoplasm and facilitate cell-to-cell dissemination[17,18,19]. They achieve that through the expression of proteins that enable them to interfere with host actin polymerization pathways and to produce actin comet tails that facilitate their forward propulsion[16,20]. As a result of infection, the host cell's actin cytoskeleton needs to dynamically rearrange in a manner that is still not fully characterized, potentially affecting the biomechanics of the host cells including the physical forces they exert on their ECM and on each other. To examine these processes, human microvascular endothelial cells (HMEC-1) were chosen as model host cells for three reasons: 1. endothelial cells are known to be highly mechanosensitive as

they are constantly exposed to varying physical cues[21]; 2. the strategies Lm employs to infect endothelial cells are still largely unknown[22]; and 3. HMEC-1 are an immortalized cell line and can, therefore, be easily cultured and subjected to genetic manipulation.

Bacterial infection of host cells has mostly been studied *in vitro* by seeding cells on glass or polystyrene substrates that are significantly stiffer than the physiological ECM of most cells[12,14,23]. To examine the infection of cells seeded on a matrix whose stiffness is physiologically relevant and to elucidate the role of ECM stiffness on the infection of cells by bacterial pathogens, we followed an innovative approach based on fabricating thin microbead-embedded polyacrylamide hydrogels of tunable stiffness on multi-well plates. The novelty of the proposed approach lies in that it allows monitoring multiple conditions simultaneously due to its multi-well format and in that it is compatible with multiple techniques due to the particular way the substrates are built. HMEC-1 cells were seeded on these protein-coated hydrogels and then infected with different Lm strains that either become fluorescent upon internalization or are constitutively fluorescent. The role of ECM stiffness on infection susceptibility of host HMEC-1 cells was evaluated by flow cytometry. In addition, immunostaining and fluorescence microscopy were used to differentiate between adhering and internalized bacteria. Finally, Traction Force Microscopy (TFM) was successfully performed to characterize the effect of Lm infection on the traction stresses that host endothelial cells exert on their matrices during infection. The presented assay can be easily modified to enable further studies on the effect of ECM stiffness on infection susceptibility of adherent cells using different cell lines or pathogens.

Protocol

1. Manufacturing Thin Two-layered Polyacrylamide (PA) Hydrogels on Multi-Well Plates

1. Dissolve ammonium persulfate (APS) in distilled ultrapure water to achieve a final concentration of 10 g/mL. Aliquot and store the solution at 4 °C for short-term use (3 weeks).
   NOTE: The above solution can be prepared in advance of hydrogel fabrication.
2. **Glass activation of 24-well dishes**
   1. Incubate 24-well glass bottom plates with 13 mm-diameter wells (see **Table of Materials**) for 1 h with 500 µL of 2 M NaOH per well at room temperature.
   2. Rinse the wells 1x with ultrapure water and then add 500 µL of 2% (3-Aminopropyl)triethoxysilane (see **Table of Materials**) in 95% ethanol to each well for 5 min.
   3. Rinse the wells 1x again with water and add 500 µL of 0.5% glutaraldehyde to each well for 30 min. Rinse the wells 1x with water and dry them at 60 °C with the lid off.
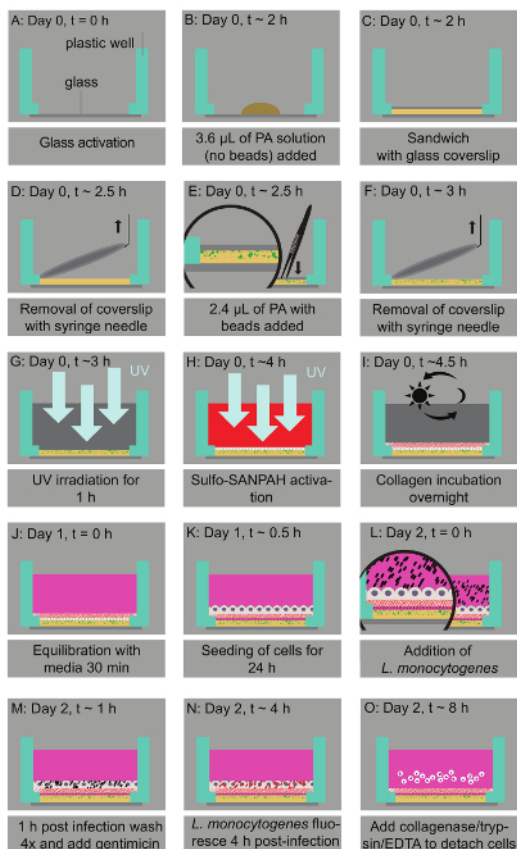
Figure 1: Bacterial infection assay of host cells residing on thin two-layered fluorescent bead-embedded polyacrylamide (PA) hydrogels of varying stiffness. A. Glass coverslips are chemically modified to enable hydrogel attachment. **B**. 3.6 µL of PA mixtures are deposited on the glass bottoms. **C**. The mixture is covered with a 12-mm circular glass coverslip to enable polymerization. **D**. The coverslip is removed with a needle syringe. **E**. 2.4 µL of a PA solution with microbeads is added on top of the bottom layer and capped with a circular glass coverslip. **F**. A buffer is added in the well and the coverslip is removed. **G**. UV irradiation for 1 h ensures sterilization. **H**. A Sulfo-SANPAH-containing solution is added on the gels, which are then placed under UV for 10 min. **I**. The hydrogels are washed with a buffer and then incubated overnight with collagen I. **J**. The hydrogel is equilibrated with cell media. **K**. The host cells are seeded. **L**. Lm bacteria are added to the solution and the infection is synchronized via centrifugation. **M**. 1 h post-infection bacteria in the solution are washed away and media supplemented with an antibiotic is added. **N**. At 4 h post-infection, Lm (JAT985) starts fluorescing. **O**. HMEC-1 cells are detached from their matrix and the solutions are transferred to tubes to perform flow cytometry measurements. Note that days and approximate times for each step of the assay are also indicated. This figure has been modified from Bastounis and Theriot[59]. Please click here to view a larger version of this figure.

3. **Polyacrylamide hydrogel fabrication**
   NOTE: See **Figure 1**.
   1. Prepare aqueous solutions that contain 3 - 10% of 40% stock acrylamide solution (see **Table of Materials**) and 0.06 - 0.6% of 2% stock bis-acrylamide solution (see **Table of Materials**) to manufacture hydrogels of tunable stiffness ranging from 0.6 kPa to 70 kPa. See **Table 1**.
      1. For 0.6 kPa hydrogels, mix 3% acrylamide with 0.045% bis-acrylamide. For 3 kPa hydrogels, mix 5% acrylamide with 0.074% bis-acrylamide. For 10 kPa hydrogels, mix 10% acrylamide with 0.075% bis-acrylamide. For 20 kPa hydrogels, mix 8% acrylamide with 0.195% bis-acrylamide. For 70 kPa hydrogels, mix 10% acrylamide with 0.45% bis-acrylamide.
         NOTE: Further details on achieving the desirable PA hydrogel stiffness can be found elsewhere[24,25,26,27].
   2. Prepare two aqueous solutions for each desirable hydrogel stiffness. Prepare Solution 1 to be bead-free and Solution 2 to contain 0.03% 0.1-µm diameter fluorescent micro-beads (see **Table of Materials**).
   3. Degas Solutions 1 and 2 by vacuum for 15 min to eliminate oxygen that is known to inhibit polymerization of the solutions.
   4. Add 0.6% of the 10 g/mL stock APS solution and 0.43% tetramethylethylenediamine (TEMED) to Solution 1 to enable a polymerization initiation. Act fast.
   5. Add 3.6 µL of Solution 1 to the center of each well of the 24-well dish (see **step 1.2** for its preparation).
   6. Immediately cover the wells with 12-mm untreated circular coverslips and let Solution 1 sit for 20 min so that it fully polymerizes.
   7. Gently tap a syringe needle to a surface to create a small hook at its tip to facilitate the removal of the coverslips. Lift the coverslips using the syringe needle.
   8. Add 0.6% of the 10 g/mL stock APS solution and 0.43% TEMED to Solution 2. Deposit 2.4 µL of the mixture on top of the first layer in each well of the 24-well dish.
   9. Cover Solution 2 with 12-mm circular glass coverslips, gently pressing downwards using a pair of forceps to ensure the thickness of the second layer is minimal. Let Solution 2 polymerize for 20 min.
   10. Add 500 µL of 50 mM HEPES pH 7.5 to each of the wells and then remove the glass coverslips with the syringe needle and forceps.

4. **Sterilization, collagen-coating, and equilibration of polyacrylamide hydrogels**
   1. UV-expose the hydrogels for 1 h in the tissue culture hood to allow sterilization.
   2. Prepare a mixture of 0.5% weight/volume sulfosuccinimidyl 6-(4′-azido-2′-nitrophenylamino)hexanoate (Sulfo-SANPAH, see **Table of Materials**) in 1% DMSO and 50 mM HEPES pH = 7.5.
   3. Add 200 µL of this solution to the upper surface of the hydrogels. Acting fast, expose them to UV (302 nm) for 10 min to activate them.
   4. Wash the hydrogels twice with 1 mL of 50 mM HEPES pH = 7.5. Repeat if needed to ensure that any excess crosslinker is removed.
   5. Protein-coat the hydrogels with 200 µL of 0.25 mg/mL rat tail Collagen I (see **Table of Materials**) in 50 mM of HEPES. Incubate the hydrogels, with the collagen solution on top, overnight at room temperature.
      NOTE: To prevent dehydration/evaporation, place the multi-well plates in a secondary containment and add laboratory cleaning tissues soaked in water in the inner periphery of the containment.
   6. Use an epifluorescence or confocal microscope with a 40X objective to measure the thickness of the hydrogels. Do so by locating the z positions of the bottom (where the glass surface is) and top planes of the hydrogel (where the fluorescent beads' intensity is maximum). Then subtract the z positions to determine the height.
      NOTE: We used an inverted epifluorescence microscope and a 40X objective with numerical aperture 0.65 to measure the thickness of the hydrogels. Atomic Force Microscopy measurements (AFM) can also be performed at this point to confirm the exact stiffness of the hydrogels (see **Figure 2**).
   7. Before seeding the cells of interest on the hydrogels, add 1 mL of media on the hydrogels and incubate them at 37 ˚C for 30 min to 1 h to ensure equilibration.
      NOTE: We added MCDB-131 full media because that is the media where the model host cells (HMEC-1) were cultured in (see **step 2.1** for details).
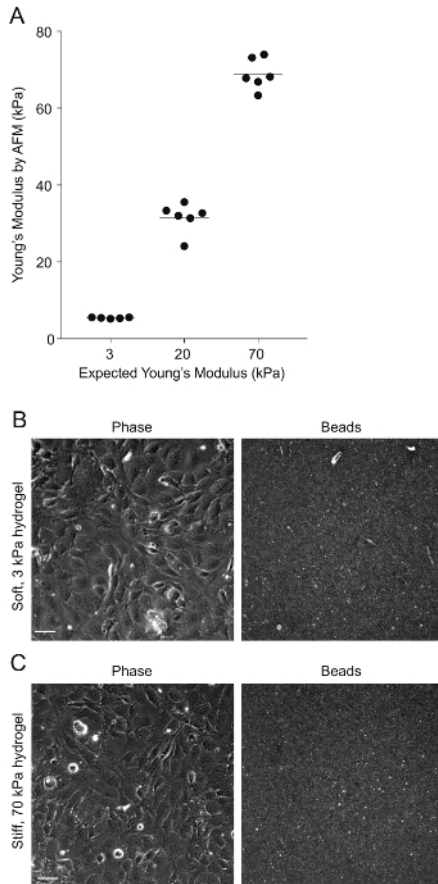
Figure 2: **AFM measurements of PA hydrogel stiffness and beads' distribution. A**. Data show the expected Young's modulus (measure of stiffness) of the PA hydrogels, given the amount of acrylamide and bis-acrylamide used versus the Young's modulus measured through AFM (N = 5 - 6). The horizontal bars depict the mean. The stiffness of the 0.6 kPa hydrogels could not be measured because the hydrogels were very soft and adhered to the AFM tip. **B**. This is a phase image of confluent HMEC-1 cells and the corresponding image of the beads embedded on the uppermost surface of a soft 3 kPa-PA hydrogel. The HMEC-1 were seeded for 24 h at a concentration of 4×10^5 cells per well. **C**. This image is the same as **Figure 2B** but for cells residing on a stiff 70-kPa PA hydrogel. Please click here to view a larger version of this figure.

2. Human Microvascular Endothelial Cell Culture and Seeding on Hydrogels

1. Culture HMEC-1 (human, microvascular endothelial) cells in MCDB-131 full media containing MCDB-131 media supplemented with 10% fetal bovine serum, 10 ng/mL of epidermal growth factor, 1 µg/mL of hydrocortisone, and 2 mM of L-glutamine (see **Table of Materials**).
2. Split the confluent cultures 1:6 every 3 - 4 days and keep the cells until passage 40.
3. One day prior to the experiment, detach the cells from their culture vessel using 0.25% trypsin/EDTA. First wash the cells and their culture vessel 1x with sterile phosphate buffered saline (PBS), and then add the appropriate amount of 0.25% trypsin/EDTA (2 mL per 100-mm dish or 75-cm flask, 1 mL per 60-mm dish or 25-cm flask), incubating the flask at 37 °C for 5 - 10 min to allow the detachment of the cells from their substrate.
4. Neutralize the trypsin by adding the desired volume of MCDB-131 full media, pipet gently to break up the clumps of cells, and then place the solution into a conical centrifuge tube.
5. Gently swirl the solution of cells to ensure that the cells are evenly distributed and then take out 20 µL of the solution and very gently fill out the two chambers underneath the coverslip of a glass hemocytometer.
6. Pellet down the solution of cells contained in the conical centrifuge tube using centrifugation for 10 min at 500 x g.
7. During the 10 min waiting period, count the cells using a hemocytometer. Use a microscope, focus on the grid lines of the hemocytometer with a 10X objective, and then use a hand tally counter to count the number of cells in one 1 mm x 1 mm square.
8. Move the hemocytometer to another 1 mm x 1 mm square, count the cells there and then repeat the process two more times. Calculate the average of the four measurements and then multiply the average by 10^4. The final value is the number of viable cells/mL in the cell suspension that is being centrifuged.
9. Remove the liquid out of the conical centrifuge tube while ensuring that the cell pellet is not disrupted. Resuspend the cells in the MCDB-131 full media at a concentration of 4×10^5 cells/mL.
10. Seed the cells in suspension on the hydrogels by first removing the media with which the hydrogels were incubated and then adding 1 mL of cell suspension on each hydrogel.

3. Infection of Human Microvascular Endothelial Cells with *L. monocytogenes*

1. **Advance preparation**
   Note: Prepare the following solutions in advance.
   1. **Streptomycin, chloramphenicol, and gentamicin stocks**
      1. Prepare 50 mg/mL of streptomycin stock solutions by weighing 0.5 g of streptomycin sulfate and dissolving it completely into 10 mL of ultrapure water.
      2. Prepare 7.5 mg/mL of chloramphenicol stock solutions by weighing 75 mg of chloramphenicol and dissolving it completely into 10 mL of 100% ethanol.
      3. Prepare 20 mg/mL of gentamicin stock solutions by weighing 0.2 g of gentamicin sulfate and dissolving it completely into 10 mL of ultrapure water.
      4. Filter-sterilize all stock solutions with a 0.2-µm syringe filter and store them at -20 °C for long-term use (1 - 2 months).

   2. **Brain heart infusion (BHI) media and agar plates**
      1. Locate two 1-L flasks and add a magnetic stir bar inside each flask.
      2. For the BHI media, add 37 g of BHI powder in one flask and add ultrapure water up to 1 L. Mix the solution vigorously by placing the flask on a magnetic stir plate until the powder is dissolved.
      3. For the BHI agar plates, add 37 g of BHI powder and 15 g of granulated agar (see **Table of Materials**) in the second flask and add ultrapure water up to 1 L. Mix the solution vigorously by placing the flask on a magnetic stir plate until the powder is dissolved.
      4. Screw the lids of the flasks not too tightly and autoclave the solutions using the liquid setting or according to the autoclave's specifications.
      5. Remove the solution from the autoclave, then cool down the agar-BHI solution to 55 °C. If the BHI media in the 1 L flask is kept sterile, it can be used for up to a month.
      6. To prepare the bacteria agar-BHI plates, first add antibiotics, if appropriate, to the flask containing BHI and agar (depending on the bacterial strains to be grown). Briefly put the flask on a magnetic stir plate to allow quick mixing.
         NOTE: The antibiotics used here are specific to the Lm strains used, but any necessary antibiotics can be used in BHI-agar plates. We added streptomycin to a concentration of 200 µg/mL and chloramphenicol to a concentration of 7.5 µg/mL because 10403S Lm strains are resistant to streptomycin. These strains have been conjugated with a plasmid that contains the chloramphenicol acetyltransferase open reading frame, hence the resistance to chloramphenicol.
      7. Pour the mixture into 10-cm polystyrene bacteria culture plates (approximately 20 mL per plate). To get rid of bubbles, flame the upper surface of the plates briefly. Cool plates overnight at room temperature.
      8. The next day, seal the dry plates and store them at 4 °C.

2. **Infection of human microvascular endothelial cells with *L. monocytogenes***
   1. Three days before the infection, streak out the Lm strain to be used from a glycerol stock (stored at -80 °C) onto a BHI-agar plate that contains 7.5 µg/mL of chloramphenicol and 200 µg/mL of streptomycin, if appropriate.
      NOTE: The strain to be streaked out can be a wild-type or mutant, constitutively expressing fluorescence (for immunostaining JAT1045 was used) or expressing fluorescence under the ActA promoter (for flow cytometry or traction force microscopy JAT983 or JAT985 were used)[22].
   2. Incubate plates at 37 °C until discrete colonies are formed (1 - 2 days).
   3. The day before the infection, grow the desired strain overnight, shaking it at 150 rpm at 30 °C in BHI media with 7.5 µg/mL of chloramphenicol (if appropriate).
      1. Place 5 mL of BHI media in a 15-mL conical centrifuge tube, add 7.5 µg/mL of chloramphenicol (if appropriate), and then inoculate a single colony from the agar plate using a sterile 10 µL tip.

   4. The next day, just prior to infection, measure the optical density of the bacteria solution at 600 nm (OD600) by diluting the sample 1:5; use a cuvette containing BHI alone to serve as a blank.
   5. Dilute the overnight culture to an OD600 of 0.1 and incubate it, shaking for 2 h at 30 °C, in BHI media with 7.5 µg/mL of chloramphenicol (if appropriate) to allow the bacteria to reach log-phase growth.
   6. Measure the OD600 of the bacterial solution, which is expected to be around 0.2 - 0.3. If the OD600 is higher, dilute it to 0.2 - 0.3 with BHI alone.
   7. Take 1 mL of bacterial solution into a microcentrifuge tube. Spin it down for 4 min at 2,000 x g using centrifugation at room temperature. Remove the supernatant and resuspend the bacterial pellet in 1 mL of tissue culture-grade PBS, in the tissue culture hood. Wash the bacteria twice more by spinning them down for 4 min at 2,000 x g at room temperature. Remove the supernatant and resuspend the bacteria in 1 mL of PBS.
   8. Prepare the infection mix by mixing 10 or 50 µL of the bacteria resuspended in PBS with 1 mL of MCDB-131 full media for a multiplicity of infection (MOI; *i.e.*, the number of bacteria per host cell) of approximately 50 bacteria per host cell or 10 bacteria per host cell.
   9. Remove the media from the wells of the 24-well plates, careful not to disrupt the hydrogels or the cells. Wash the cells 1x with 1 mL of MCDB-131 full media and then add 1 mL of the bacteria to each well.
   10. Keep some infection mix (at least 100 µL) for the determination of MOI (see **step 3.3**).
   11. Cover the plate with its lid and wrap the plates with polyethylene food wrap to avoid leakage. Place the plates in the centrifuge and spin the samples for 10 min at 200 x g to synchronize the invasion. Move the plates into the tissue culture incubator and incubate them for 30 min at 37 °C.
   12. Wash the samples 4x with MCDB-131 full media and move them into the tissue culture incubator. After an additional 30 min, replace the media with media supplemented with 20 µg/mL of gentamicin.

3. **Determination of the multiplicity of infection (MOI)**

1. During the initial 30-min incubation of the host cells with the bacteria, prepare 10-fold serial dilutions of the infection mix to determine the MOI. Make 10-fold dilutions by mixing 100 µL of the infection mix with 900 µL of 1x PBS (10^{-1} dilution). Then, mix 100 µL of the 10^{-1} dilution with 900 µL of PBS (10^{-2} dilution).
2. Continue until a 10^{-5} dilution is obtained.
   NOTE: All solutions need to be mixed well before diluting them, and fresh clean pipette tips should be used at each step.
3. Once the dilutions are made, place 100 µL of the 10^{-2} - 10^{-5} dilutions on the center of the BHI/agar/chloramphenicol/streptomycin plates (if appropriate).
4. Make a spreader from a glass pipette by using fire to bend the pipette to create a hook. Dip the pipette in 100% ethanol for sterilization and then burn off the ethanol with a flame.
5. Once the spreader has cooled, spread the bacterial dilutions homogeneously on the plates starting from the 10^{-5} dilution and moving to the more concentrated mixes. Incubate the plates upside down at 37 °C for 2 days.
6. Depending on the colony density, determine the number of colonies of either the 10^{-3} and 10^{-4} or the 10^{-4} and 10^{-5} dilution plates. Calculate the MOI as follows:
   number of colonies × dilution factor ÷ volume initial added = number of CFU per µL
   number of CFU per µL × volume of bacteria mix per well = number of CFU per well
   number of CFU per well × volume of cells per well = number of bacteria per cell
   NOTE: CFU stands for colony-forming units.
7. Average the MOIs from two plates to obtain the final MOIs.

4. Flow Cytometry to Quantify Extracellular-matrix-stiffness Dependent Susceptibility of Host Cells to Infection

1. Weigh 5 mg of collagenase and place it in a 15-mL conical centrifuge tube. Add 10 mL of 0.25% trypsin-EDTA and mix them well.
2. 8 h post-infection, remove the media from the wells of the 24-well plate and wash the wells 1x with tissue culture PBS. Remove the PBS from the wells and add 200 µL of the trypsin-EDTA/collagenase mix to each well. Place this in the tissue culture incubator for 10 min to allow full detachment of the cells.
3. Use a fresh pipette for each well and pipet the mix up and down 8x. Be gentle so as to not damage the cells. Add 200 µL of full media to each well to neutralize the trypsin.
4. Transfer the 400-µL cell solution of each well into a 5-mL polystyrene tube with a 35-µm cell strainer cap (see **Table of Materials**).
5. Analyze 10,000 - 20,000 cells per sample by flow cytometry. Perform data acquisition through flow cytometry and determine the percentage of infected cells per well using a relevant commercially-available software. Use the forward scatter versus side scatter plots to gate the bulk of the distribution of the cell counts.
   NOTE: This will ensure analysis of single cells and eliminate debris or cell doublets or triplets.
   1. Measure the fluorescence signal from control-uninfected cells and gate the population of infected cells excluding autofluorescence.

5. Immunostaining of the Extracellular Bacteria, Microscopy and Image Processing

Note: This approach is followed to differentiate between ECM-stiffness dependent bacterial adhesion onto the host cell surface versus bacterial internalization (invasion) within the hosts.
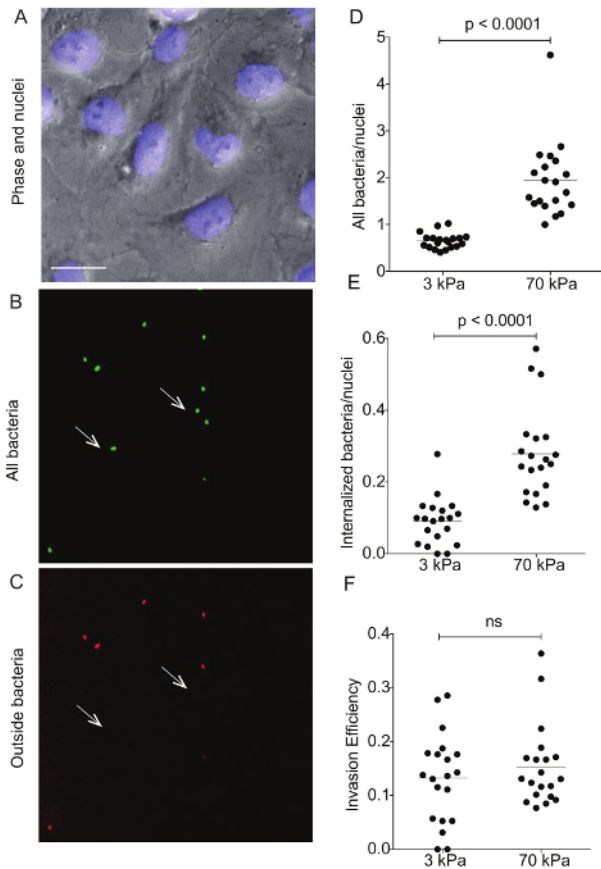
Figure 4: Immunostaining of Lm-infected HMEC-1 cells residing on hydrogels of varying stiffness to differentiate bacterial adhesion versus invasion. These images show a representative example of differential immunostaining showing **A**. the cell nuclei (DAPI), **B**. all bacteria (GFP), and **C**. the outside bacteria (Alexa-546). The HMEC-1 cells were residing on a soft 3-kPa hydrogel. The arrows point at bacteria that have been internalized, so are shown on the green channel only. Data in **D-F** refer to N = 20 images captured for the infected HMEC-1 cells residing on soft 3-kPa and stiff 70-kPa hydrogels and **show D**. the total bacteria per nuclei; **E**. the internalized bacteria per nuclei; **and F**. the invasion efficiency (the ratio of internalized bacteria to total bacteria). The horizontal bars depict the data's mean. The *P*-value was calculated with the non-parametric Wilcoxon Rank Sum test. Please click here to view a larger version of this figure.

1. 30 min post-infection, wash the HMEC-1 cells infected with JAT1045 (Lm that constitutively expresses green fluorescent protein (GFP)) 4x with media.
2. After the fourth wash, mix 1 µL of 1 mg/mL Hoechst dye with 1 mL of MCDB-131 full media and add it to each well to stain the cells' nuclei. Place the cells in the tissue culture incubator for 10 min.
3. Wash the cells 1x with PBS. Fix them with a non-permeabilizing fixative for differential immunostaining for 20 min at room temperature[28]. NOTE: The fixative contains 0.32 M sucrose, 10 mM MES pH 6.1, 138 mM KCl, 3 mM $MgCl_2$, 2 mM EGTA, and 4% formaldehyde (electron microscopy grade).
4. Wash the cells 1x with PBS. Block the samples for 30 min with 5% bovine serum albumin (see **Table of Materials**) in PBS.
5. Incubate the samples for 1 h with an anti-Lm*primary antibody (see* **Table of Materials**) diluted 1:100 in PBS containing 2% BSA.
6. Wash the samples in PBS 3x and then incubate them for 1 h with an AlexaFluor-546 goat-anti-rabbit secondary antibody (see **Table of Materials**) diluted 1:250 in PBS containing 2% BSA. Wash the samples 3x in PBS. Store the samples in 1 mL of PBS for imaging.
7. Image and analyze more than 1,000 cells per condition.
   1. For imaging, use an inverted epifluorescence microscope with a CCD camera (see **Table of Materials**) and a 40X air plan fluorite air objective with 0.6 numerical aperture (NA). NOTE: The power is set to 25% and the exposure time to 100 ms. The microscope filters used for mCherry are 470/525 nm, for GFP 530/645 nm, and for DAPI 395/460 nm, for excitation and emission respectively. The microscope we used was controlled by an open source microscopy software package[29].
   2. For differential immunostaining, count all 'green' bacteria associated with individual cells as adherent. Count bacteria that are both 'green' and 'red' (due to antibody binding) as non-internalized. NOTE: We identified the nuclei number by running a custom-made script and the CellC software (see **Table of Materials**) for enumeration of the bacteria[30].

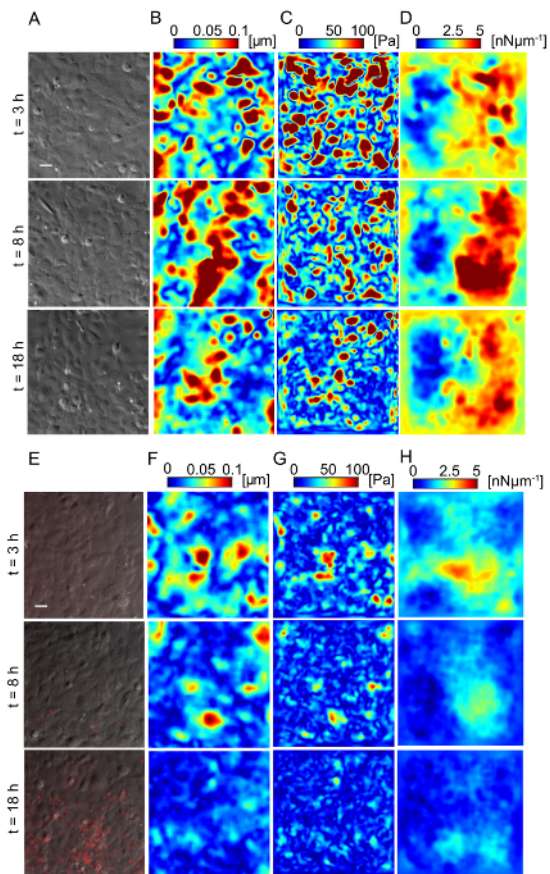## 6. Multi-well Traction Force Microscopy and Monolayer Stress Microscopy

Figure 5: **Lm-infected HMEC-1 cells decrease the magnitude of the traction forces they exert on their ECM during infection.** Panel **A** shows the phase image, **B** shows the deformation field, **C** shows the traction stress field, and **D** shows the intracellular tension field of the uninfected HMEC-1 cells residing on a 20-kPa hydrogel. The color bars of the deformation maps (μm), of the traction stress maps (Pa), and of the intracellular tension maps (nNμm^{-1}) are shown on the upper portion of the heat maps. The columns show three representative time points: 3, 8 and 18 h post-infection. **E-H**. Same as panels **A-D** but for cells infected with Lm at an MOI of 300. The images of the bacteria (red channel) are superimposed on the phase images of the cells. TFM recordings were conducted by imaging multiple wells simultaneously. The window size for PIV was 32 pixels with an overlap of 16. The scale bar is 32 μm. This figure has been modified from Bastounis and Theriot[59]. Please click here to view a larger version of this figure.

1. Prepare the PA hydrogels on a 24-well plate (see **step 1**). Seed HMEC-1 cells (see **step 2**) and infect them with JAT983 as described above (see **step 3**).
2. Prepare a live-microscopy medium by supplementing Leibovitz's L-15 with 10% fetal bovine serum, 10 ng/mL of epidermal growth factor, and 1 μg/mL hydrocortisone.
   NOTE: The L-15 already contains 2 mM L-glutamine, so it is not necessary to add extra as in the case of MCDB-131 media.
3. 4 h post-infection (when the internalized JAT983 starts fluorescing), mix 1 μL of 1 mg/mL Hoechst dye with 1 mL of L-15 full media and add it to each well to stain the cells' nuclei. Place the cells in the tissue culture incubator for 10 min and then replace in each well the L-15 full media with 1 mL of L-15 full media supplemented with 20 μg/mL of gentamicin.
4. Cover the plate with its lid and place it in a microscope's environmental chamber (see **Table of Materials**) equilibrated to 37 ˚C.
   NOTE: For imaging, use an inverted epifluorescence microscope with a CCD camera (see **Table of Materials**) and a 40X air plan fluorite air objective with 0.6 NA.
5. Acquire multi-channel time-lapse images of the fluorescent beads and the fluorescent bacteria, and phase contrast images of the host cells, every 10 min for 4 to 12 h.
   NOTE: For the imaging, the power was set to 25% and the exposure time to 100 ms. The microscope filters (excitation/emission) used for mCherry and GFP are 470/525 nm and 530/645 nm respectively.
6. At the end of the recording, add 500 μL of 10% sodium dodecyl sulfate (SDS) in water in each of the wells.
   NOTE: The cells will be detached from the hydrogel and the hydrogel will return to its initial undeformed state since it is elastic.
7. Take an image of the hydrogel and use it as the reference undeformed image.
8. Determine the two-dimensional deformation of the hydrogel at each instant of time using particle image velocimetry (PIV)[31], comparing each image of the time-lapse series with the reference image of the undeformed hydrogel. Use the appropriate window sizes and overlap depending on the experiment.
   NOTE: We used windows of 32 pixels with an overlap of 16 pixels.
9. Calculate the 2D traction stresses that cells exert on the hydrogel as described elsewhere[32,33].

10. Calculate the monolayer tension from the traction stresses as previously described[34] by solving the equations of mechanical equilibrium for a thin elastic plate subject to the reaction forces created by the PA hydrogel on the monolayer, which are of an opposite sign to the measured traction stresses.
NOTE: See **Supplementary Material 1**.

7. Quantitative Time-lapse Microscopy to Assess Extracellular-matrix-stiffness Dependent *L. monocytogenes* Dissemination Through Endothelial Cells
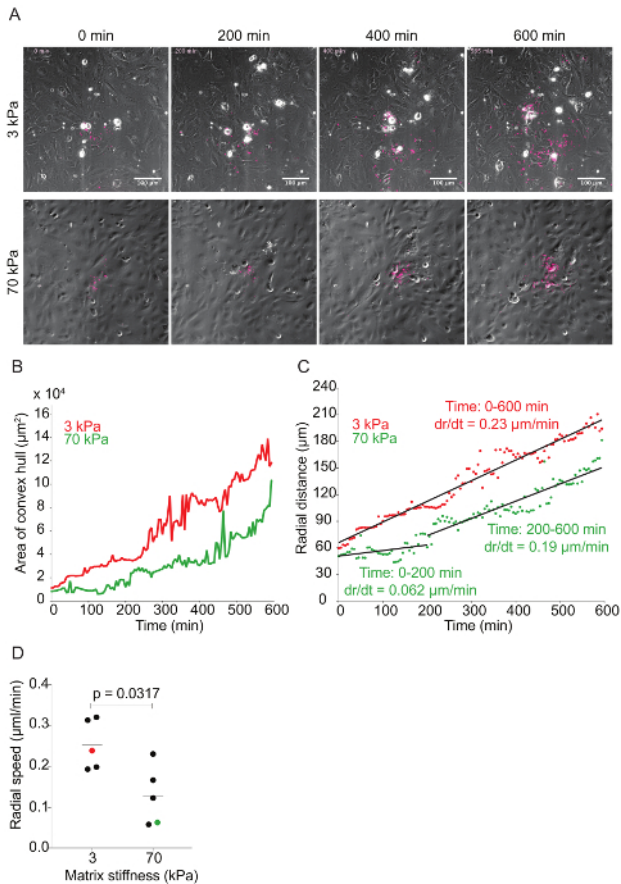

Figure 6: **Time-lapse quantitative microscopy data of Lm dissemination through HMEC-1 monolayers seeded on substrates with 3-kPa and 70-kPa stiffness. A.** This panel shows still images from two representative infection foci at 0, 200, 400, and 600 min. The phase channel depicts HMEC-1 cell monolayers, and the red channel depicts intracellular Lm (see **step 7** of the protocol). **B.** This panel shows the area of the convex hull encompassing the infection focus plotted as a function of time. The focus area of the 3-kPa condition (red) grows faster than that of the 70-kPa (green). **C.** This panel shows the radial distance from the center to the edge of the infection focus plotted as a function of time for representative infection foci growing in HMEC-1 monolayers seeded on PA substrates of 3-kPa (red) and 70-kPa (green) stiffness. The radial speed (dr/dt) is constant for the 3-kPa condition, but biphasic for the 70-kPa condition. **D.** These data show the radial speed for the first 200 min of ten independent infection foci. The red (3-kPa) and green (70-kPa) data points depict the slopes of the two foci described in the previous panels. The horizontal bars depict the data's mean. The *P*-value was calculated with the non-parametric Wilcoxon Rank Sum test. Please click here to view a larger version of this figure.

1. Prepare the PA hydrogels on a 24-well plate (see **step 1**), seed HMEC-1 cells (see **step 2**), and grow overnight JAT983 cultures as described above (see **step 3**).
2. The day of infection, prepare the infection mix by mixing 10 µL of bacterial pellet per mL of MCDB-131 full media. Carefully remove the media from the wells of the 24-well plates, and add 1.9 mL of the MCDB-131 full media and 0.1 mL of the bacterial mix to each well.
NOTE: The lower MOI used in this assay is necessary to analyze dissemination events that start from a single bacterium invading a host cell.
3. Cover the plate with its lid and seal it with a plastic wrap to avoid leakage. Place the plates in the centrifuge and spin the samples for 10 min at 200 x g to synchronize the invasion.
4. Move the plates into the tissue culture incubator and incubate them for 5 min.
5. Wash the samples 4x with media and move them to the tissue culture incubator. After an additional 5 - 7 min, replace the media with media supplemented with 20 µg/mL of gentamicin.
6. Incubate the plate in the incubator for an extra 5 h to allow the actA promoter to turn on and drive the expression of the mTagRFP open reading frame[35].
7. Prepare a live-microscopy medium by supplementing Leibovitz's L-15 with 10% fetal bovine serum, 10 ng/mL of epidermal growth factor, and 1 µg/mL hydrocortisone.

NOTE: The L-15 already contains 2 mM L-glutamine, so it is not necessary to add extra as in the case of MCDB-131 media.

8. Mix 1 µL of 1 mg/mL Hoechst dye with 1 mL of L-15 full media and add it to each well to stain the cells' nuclei. Place the cells in the tissue culture incubator for 10 min and then replace in each well the L-15 full media with 1 mL of L-15 full media supplemented with 20 µg/mL of gentamicin. Cover the plate with its lid and place it in a microscope's environmental chamber (see **Table of Materials**) equilibrated to 37 ˚C.
    NOTE: For imaging, an inverted epifluorescence microscope was used with a CCD camera (see **Table of Materials**) and a 20X air plan fluorite air objective with 0.75 NA. The power was set to 50% and the exposure time to 50 ms. The microscope filters used for mCherry are 470/525 nm for excitation and emission respectively.
9. Image multiple positions every 5 min using an autofocus feature to monitor how Lm spread through HMEC-1 monolayers seeded on varying stiffness hydrogels.
    NOTE: L-15 is buffered with HEPES, so it is not necessary to use CO_2 during the imaging.

Representative Results

ECM stiffness-dependent susceptibility of HMEC-1 cells to Lm infection:
PA hydrogels of varying stiffness, all surface-coated with collagen I, were built on multi-well glass bottom plates as described in **step 1** of the protocol (see **Figure 1**). AFM measurements were performed to confirm the exact stiffness of the hydrogels, as described previously[26,27] (see **Figure 2**). Past studies have shown that the local compliance of the basement membrane of endothelial cells can range from 1 kPa (*e.g.*, brain tissue) to 70 kPa (*e.g.*, aorta)[36,37,38,39,40]. Therefore, we chose to test the infection of HMEC-1 cells residing on matrices with the following stiffness: 0.6 kPa, 3 kPa, 20 kPa, and 70 kPa. For each hydrogel stiffness, six hydrogels were fabricated to assess the reproducibility of the results.

Flow cytometry was used to assess the ECM stiffness-dependent susceptibility of HMEC-1 cells to Lm infection (see **Figure 3**). HMEC-1 cells were infected with a Lm strain (JAT985) that expresses a fluorescent marker after internalization (actAp::mTagRFP), allowing the detection of intracellular bacteria only (see **Figures 1L** - **1N**). JAT985 also lacks ActA, disabling the bacteria from spreading from cell to cell, since ActA is necessary for the formation of actin comet tails and subsequent bacterial dissemination. 7 - 8 h post-infection, the HMEC-1 cells' infection was assessed using flow cytometry. To ensure the analysis of single cells, the bulk of the distribution of cell counts was gated using the forward versus side scatter plot, and then a second gating step was performed to exclude cells that exhibit autofluorescence (see **Figures 3A** - **3C**). The preliminary results depicted in **Figure 3** show that HMEC-1 infection with Lm is approximately two-fold greater for HMEC-1 cells residing on the stiff 70 kPa hydrogels as compared to cells residing on the soft 0.6 kPa hydrogels (see **Figures 3B** - **3D**). The increased Lm infection susceptibility of HMEC-1 cells residing on stiff as compared to soft matrices could be due to: 1. increased Lm adhesion onto HMEC-1; 2. increased Lm invasion into HMEC-1; or 3. both of the above co-occurring. To test which hypothesis holds, HMEC-1 cells were seeded on soft (3 kPa) and stiff (70 kPa) hydrogels and infected with constitutively GFP expressing Lm (see **Figures 4A** - **4C**). The samples were fixed shortly after infection and the external (adhering) bacteria were stained with antibodies. Using quantitative microscopy, we found that there are significantly more bacteria adhering to HMEC-1 when the host cells reside on stiff as compared to soft gels (see **Figure 4D**). Consistent with the flow cytometry data, there are significantly more bacteria internalized by HMEC-1 when the host cells reside on stiff as compared to soft gels (see **Figure 4E**). However, the invasion efficiency (bacteria internalized/total number of bacteria) of Lm into HMEC-1 cells is similar, irrespective of substrate stiffness (see **Figure 4F**).

Traction force microscopy of Lm-infected HMEC-1 cells:
Lm infection of HMEC-1 cells could alter the biomechanics of infected host cells, including the strength of attachment to their ECM or to each other, affecting their barrier integrity. We sought to evaluate whether that could be the case by using Traction Force Microscopy[32] to calculate the cell-ECM traction forces and Monolayer Stress Microscopy[41] to calculate the intracellular tensional forces. **Figure 5** depicts maps of the deformation field, traction stress field, and intracellular tension field of HMEC-1 cells residing on 20-kPa hydrogels at different time points post-infection. **Figures 5A** - **5D** refer to uninfected control HMEC-1 cells while **Figures 5E** - **5H** refer to HMEC-1 cells infected with Lm at a multiplicity of infection equal to 300 bacteria/cell. This preliminary work suggests that infected HMEC-1 cells reduce the magnitude of their cell-ECM and intracellular stresses during the course of an infection with Lm, whereas that is not observed for uninfected control cells.

ECM stiffness-dependent Lm dissemination across HMEC-1 monolayers:
Time-lapse microscopy was used to investigate the effect matrix stiffness has on Lm dissemination through HMEC-1 monolayers. As Lm spreads through the monolayer, the bacteria create a focus of infection that grows as a function of time (see **Figure 6A** and **Video Figures 1** and **2**). The area of the infection focus was measured by drawing a convex hull, the smallest convex polygon that encompasses a set of points, around the bacteria[42]. There is no standard metric in the field to measure the efficiency of *L. monocytogenes* cell-to-cell spread through a monolayer of host cells. To assess spread efficiency, some have counted the number of host cells in an infection focus[41], and others have drawn boundaries manually around the group of infection host cells[43]. We chose to draw a convex polygon around the bacteria, because it is an automated, consistent, and computationally inexpensive process to measure the efficiency of *L. monocytogenes* spread. By doing so, we found a slight decrease in the infection focus area in the HMEC-1 cells seeded onto 70 kPa hydrogels when compared to those seeded on 3 kPa matrices (see **Figure 6B** and **Video Figures 1** and **2**). To determine the rate of growth of the infection focus, the radial distance was plotted as a function of time by taking the square root of the area of the infection focus and dividing this by pi. This mathematical transformation assumes that the shape of the infection focus is roughly circular[44]. To measure the speed of the focus growth, the rate of change (*i.e.*, the slope) of the radial distance for both 3- and 70-kPa matrices was measured. This approach elucidated that the infection focus grew faster and monotonically in HMEC-1 cells seeded onto 3-kPa matrices. However, the focus grew significantly slower (first 200 min) and slightly slower (200 to 600 min) in cells seeded onto 70-kPa matrices (see **Figure 6C**). Indeed, analysis of further data confirmed that the infection focus grew, on average, two-fold slower in 70-kPa matrices, especially during the first 200 min (see **Figure 6D**).
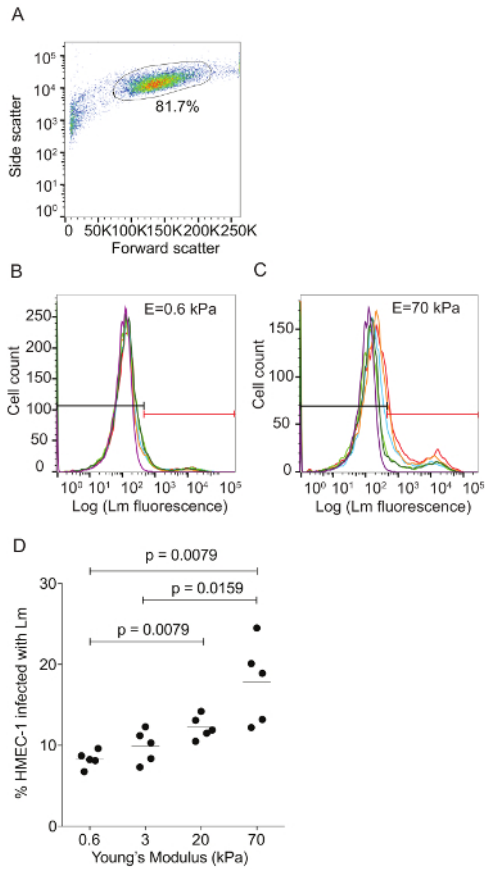
Figure 3: ECM stiffness-dependent susceptibility of HMEC-1 cells to Lm invasion measured by using flow cytometry. HMEC-1 cells were infected with Lm (JAT985) and the infection was analyzed by flow cytometry. **A**. This panel shows a side versus forward scatter plot for representative HMEC-1 cells coming from a single well. The bulk distribution of cells was selected via gating to exclude debris (left) and cell doublets or triplets (right). **B**. This graph shows a histogram of the logarithm of the Lm fluorescence intensity per cell for HMEC-1 plated on soft 0.6 kPa. **C**. This graph shows a histogram of the logarithm of the Lm fluorescence intensity per cell for HMEC-1 plated on stiff 70 kPa hydrogels. The histograms for N = 4 - 6 replicates are shown in different colors. The control uninfected cells' histogram is purple. The gate used to define what is infected is shown in red. The MOI is 100 and the infection was assessed 8 h post-infection. **D**. Data show percentage of infected HMEC-1 cells versus hydrogel stiffness (N = 5). The horizontal bars depict the data's mean. The *P*-value was calculated with the non-parametric Wilcoxon Rank Sum test. Please click here to view a larger version of this figure.
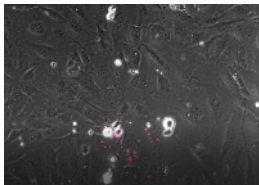

Video Figure 1: Dissemination of intracellular Lm (red channel) through an HMEC-1 cell monolayer (phase) seeded on a 3-kPa substrate. The cells were imaged in Leibovitz's L-15 media (10% FBS, 20 μg/mL of gentamicin) inside an environmental chamber equilibrated to 37 ˚C. The images were collected every 5 min. The movie speed is 15 frames/s. Please click here to view this video. (Right-click to download.)
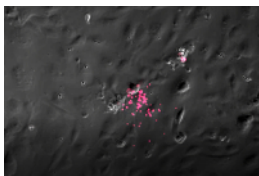
Video Figure 2: Dissemination of intracellular Lm (red channel) through an HMEC-1 cell monolayer (phase) seeded on a 70-kPa substrate. The cells were imaged in Leibovitz's L-15 media (10% FBS, 20 μg/mL of gentamicin) inside an environmental chamber equilibrated to 37 °C. The images were collected every 5 min. The movie speed is 15 frames/s. Please click here to view this video. (Right-click to download.)

Young's modulus (E, kPa)	Acrylamide % (from 40% stock)	Bisacrylamide % (from 2% stock)
0.6	3	0.045
3	5	0.075
10	10	0.075
20	8	0.195
70	10	0.45

Table 1. Composition of polyacrylamide (PA) hydrogels of varying stiffness. In this table, the percentage of stock 40% acrylamide solution and the percentage of stock 2% bis-acrylamide solution to achieve a given stiffness (Young's modulus, E) are indicated in different columns.
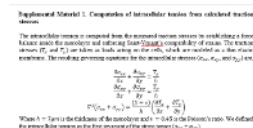
Supplemental Material 1. Computation of intracellular tension from calculated traction stresses. Please click here to download this file.

Discussion

Cells can sense a variety of physical environmental cues, which can affect not only the cells' morphology but also their gene expression and protein activity, thus affecting critical cell functions and behaviors[45,46]. The stiffness of the ECM of cells is increasingly appreciated as an important modulator of cellular motility, differentiation, proliferation, and ultimately cell fate[47,48,49]. Although there have been many recent advances in understanding the complex biomechanical interaction between cells and their ECM, little is known about how environmental stiffness affects the susceptibility of cells to bacterial infection. To facilitate such studies, we developed this novel multi-well assay based on the well-established fabrication of polyacrylamide hydrogels of tunable stiffness which is compatible with infection assays[50]. Traditionally, a bacterial infection of cells in tissue culture has been studied on glass or polystyrene surfaces that are approximately 1 - 3 orders of magnitude stiffer than the natural ECM of most adherent cells[8,51]. The assay described here opens new highways by enabling the study of bacteria-host interactions in a physiologically relevant environmental stiffness regime.

For proof of concept of the presented assay, HMEC-1 cells were chosen as model adherent host cells and Lm as a model bacterial pathogen. However, the assay can be extended for further studies if appropriately modified. Such studies can involve infection of different mammalian adherent host cell types by additional pathogens, including bacteria and viruses. For this particular assay, gels were protein-coated with collagen I, but depending on the host cell type, it is possible to use a different ECM protein-coating, such as laminin or fibronectin, to facilitate the attachment of the host cells of interest on the hydrogel[52]. An additional consideration that depends on the host cell type is the hydrogel stiffness range to be studied. The range of stiffness should depend on what is physiologically relevant for the specific host cell type and how well that host attaches forming a monolayer at a given stiffness hydrogel. Similarly, depending on the model pathogen desired to be examined, slight modifications might need to be implemented on the infection assay described herein.

The innovation of the assay as compared to previous methods for manufacturing polyacrylamide hydrogels[24,50,53] lies in certain unique features integrated into the proposed infection assay. First, the hydrogels are built on multi-well glass bottom plates, which enables the screening of multiple conditions simultaneously as well as the automation of certain procedures. Monitoring multiple conditions at the same time or examining multiple replicates is crucial since the outcome of such an approach can be influenced by factors such as the host cell passage and the precise number of bacteria added to infect the hosts, which often change between independent experiments. An additional unique feature of this assay is that the hydrogels have a height of approximately 40 μm, which is thin enough to image using conventional microscopy. We showed that we can successfully perform both live cell microscopy and cell fixation, and immunostaining followed by imaging, without introducing high background fluorescence. Lastly, the hydrogels are made of two layers, with the upper one having embedded fluorescent microbeads, confined in a single focal plane. This attribute ensures that there will be no out-of-focus light interfering during imaging. The presence of the beads enables both the examination of the surface topography of the gels to ensure that they are uniform and improves the performance of TFM and MSM[24,32,41]. With TFM and MSM, it is possible to calculate the cell-ECM and cell-cell forces respectively of cells residing on varying stiffness matrices. Using this novel assay, it is possible to make such measurements of physical forces by comparing both the contribution of environmental stiffness and of infection simultaneously. Following such an approach, the effect infection has on host cell mechanics throughout its course can be determined. Additionally, the evolution of the intracellular stresses of cells can be calculated using MSM and can be used as a measure of the barrier integrity of the monolayer. Finally, given the multi-well nature of the assay, it is possible to simultaneously introduce pharmacological and genetic perturbations with a bacterial infection, to investigate in more depth the complex interplay between host cell mechanics and infection.

One inherent limitation of the technique lies in the effect substrate stiffness might have on the proliferation rate of cells. Typically, in infection assays, we need to ensure that the host cell density under different conditions is the same. That is because cell density by itself can have an effect on the susceptibility of hosts to infection. The HMEC-1 cells that were used as host cells do not show a significant difference in their number when seeded for 24 h on the hydrogels. However, different cell types might exhibit differential proliferation, depending on the hydrogel stiffness, that can bias infection studies. Similarly, infection bias can arise when cells do not form monolayers or do not attach well on the hydrogels, as occurs when certain cell types are seeded on very soft matrices (*e.g.*, human umbilical cord endothelial cells or Madin-Darby canine kidney epithelial cells seeded on 0.6-kPa hydrogels[54,55]). As far as pathogens are concerned, certain bacteria (*e.g.*, *Borrelia burgdorferi*) can attach onto host cells and invade them but can also transmigrate through them[56]. We have not yet tested if this assay would work for pathogen transmigration studies, but it seems possible since previous studies on neutrophils transmigrating endothelial cells seeded on PA hydrogels have been documented to work successfully[57]. There have been a lot of studies conducted showing how to manufacture polyacrylamide hydrogels of a given Young's modulus by mixing the appropriate concentrations of acrylamide and bis-acrylamide[24,25,26,27].

However, especially when one desires to perform TFM experiments on cells residing on hydrogels of varying stiffness, it is critical to confirm the expected stiffness of the hydrogels either through AFM or other indentation techniques[58]. Slight deviations from the expected value can arise due to a different solvent used or an aged acrylamide stock solution, or by the ways AFM measurements are performed (*e.g.*, the shape of the AFM tip). Finally, the approach presented herein is based on seeding host cells on 2D matrices, which can differ from a more realistic and physiologically relevant 3D scenario. However, manufacturing 3D gels with tunable stiffness, seeding them with host cells and then infecting them with pathogens, still encompasses certain technical difficulties. Nevertheless, we anticipate that in the near future we will be able to extend the current assay for studying infection in a 3D setting.

To sum up, the described protocol together with the preliminary results provide evidence that this novel assay can become an extremely useful tool for studying infection of adherent host cells with pathogenic bacteria in a quantitative fashion and in a much more physiologically relevant environment than previously examined. The power of fabricating polyacrylamide hydrogels in the proposed setup lies in that the assay is compatible with the performance of multiple techniques such as flow cytometry, immunostaining followed by light microscopy, and traction force microscopy. The assay can be used for studies involving the infection of different adherent host cell types by pathogens, which we anticipate will have a significant impact in both unraveling the strategies by which pathogens infect hosts and in facilitating the development of therapeutic interventions against infections.

Disclosures

The authors have nothing to disclose.

Acknowledgements

References

1. Humphrey, J. D., Dufresne, E. R., Schwartz, M. A. Mechanotransduction and extracellular matrix homeostasis. *Nature Reviews Molecular Cell Biology.* **15** (12), 802-812 (2014).
2. Gattazzo, F., Urciuolo, A., Bonaldo, P. Extracellular matrix: a dynamic microenvironment for stem cell niche. *Biochimica et Biophysica Acta.* **1840** (8), 2506-2519 (2014).
3. Trepat, X., Lenormand, G., Fredberg, J. J. Universality in cell mechanics. *Soft Matter.* **4** (9), 1750-1759 (2008).
4. Maruthamuthu, V., Sabass, B., Schwarz, U. S., Gardel, M. L. Cell-ECM traction force modulates endogenous tension at cell-cell contacts. *Proceedings of the National Academy of Sciences of the United States of America.* **108** (12), 4708-4713 (2011).
5. Fujiwara, I., Suetsugu, S., Uemura, S., Takenawa, T., Ishiwata, S. Visualization and force measurement of branching by Arp2/3 complex and N-WASP in actin filament. *Biochemical and Biophysical Research Communications.* **293**, 1550-1555 (2002).
6. Ingber, D. E. Tensegrity-based mechanosensing from macro to micro. *Progress in Biophysics and Molecular Biology.* **97** (2-3), 163-79 (2008).
7. LaValley, D. J., Zanotelli, M. R., Bordeleau, F., Wang, W., Schwager, S. C., Reinhart-King, C.A. Matrix stiffness enhances VEGFR-2 internalization, signaling, and proliferation in endothelial cells. *Convergent Science Physical Oncology.* **3** (4), 044001 (2017).
8. Mason, B. N., Califano, J. P., Reinhart-King, C. A. Matrix stiffness: a regulator of cellular behavior and tissue formation. In *Engineering Biomaterials for Regenerative Medicine: Novel Technologies for Clinical Applications.*, edited by Bhatia, Sujata K., 19-37, Springer New York. New York, NY (2012).
9. El-Mohri, H., Wu, Y., Mohanty, S., Ghosh, G., Impact of matrix stiffness on fibroblast function. *Materials Science and Engineering: C.* **74** (Supplement C), 146-151 (2017).
10. Asano, S., *et al.* Matrix stiffness regulates migration of human lung fibroblasts. *Physiological Reports.* **5** (9), (2017).
11. Burgess, J. K., Mauad, T., Tjin, G., Karlsson, J. C., Westergren-Thorsson, G. The extracellular matrix: the under-recognized element in lung disease? *The Journal of Pathology.* **240** (4), 397-409 (2016).
12. Vazquez-Boland, J. A., *et al.Listeria.* pathogenesis and molecular virulence determinants. *Clinical Microbiology Reviews.* **14** (3), 584-640 (2001).
13. Jackson, K. A., Iwamoto, M., Swerdlow, D. Pregnancy-associated listeriosis. *Epidemiology and Infection.* **138** (10), 1503-9 (2010).
14. Theriot, J., Rengarajan, M. Exploitation of host cell processes for bacterial cell-to-cell spread. *The FASEB Journal.* **28** (1 Supplement), (2014).
15. Pollard, T. D., Beltzner, C. C. Structure and function of the Arp2/3 complex. *Current Opinion in Structural Biology.* **12** (6), 768-774 (2002).
16. Pollard, T. D. Cellular motility powered by actin filament assembly and disassembly. *Harvey Lectures.* **98**, 1-17 (2002).
17. Reed, S. C., Lamason, R. L., Risca, V. I., Abernathy, E., Welch, M. D. Rickettsia actin-based motility occurs in distinct phases mediated by different actin nucleators. *Current Biology.* **24** (1), 98-103 (2014).
18. Gerbal, F., Chaikin, P., Rabin, Y., Prost, J. An elastic analysis of *Listeria monocytogenes.* propulsion. *Biophysical Journal.* **79**. (5), 2259-2275 (2000).
19. Weber, I. Is there a pilot in a pseudopod? *European Journal of Cell Biology.* **85** (9-10), 915-924 (2006).
20. Theriot, J. A., Rosenblatt, J., Portnoy, D. A., Goldschmidt-Clermont, P. J., Mitchison, T. J. Involvement of profilin in the actin-based motility of *L. monocytogenes.* in cells and in cell-free extracts. *Cell.* **76** (3), 505-17 (1994).
21. Kohn, J. C., *et al.* Cooperative effects of matrix stiffness and fluid shear stress on endothelial cell behavior. *Biophysical Journal.* **108** (3), 471-478 (2015).
22. Rengarajan, M., Hayer, A., Theriot, J. A. Endothelial cells use a formin-dependent phagocytosis-like process to internalize the bacterium *Listeria monocytogenes. PLoS Pathogens.* **12** (5), e1005603 (2016).

July 2018 | 137 | e57361 | Page 13 of 14

23. Rajabian, T., *et al.* The bacterial virulence factor InlC perturbs apical cell junctions and promotes cell-to-cell spread of *Listeria. Nature Cell Biology.* **11**. (10), 1212-8 (2009).

24. Bastounis, E., *et al.* Both contractile axial and lateral traction force dynamics drive amoeboid cell motility. *The Journal of Cell Biology.* **204** (6), 1045-1061 (2014).

25. Georges, P., Miller, W., Meaney, D., Sawyer, E., Janmey, P. A. Matrices with compliance comparable to that of brain tissue select neuronal over glial growth in mixed cortical cultures. *Biophysical Journal.* **90** (8), 3012-3018 (2006).

26. Vincent, L. G., Choi, Y. S., Alonso-Latorre, B., del Alamo, J. C., Engler, A. J. Mesenchymal stem cell durotaxis depends on substrate stiffness gradient strength. *Biotechnology Journal.* **8** (4), 472-84 (2013).

27. Engler, A., Bacakova, L., Newman, C., Hategan, A., Griffin, M., Discher, D. Substrate compliance versus ligand density in cell on gel responses. *Biophysical Journal.* **86.** (1), 617-628 (2004).

28. Yam, P. T., Theriot, J. A. Repeated cycles of rapid actin assembly and disassembly on epithelial cell phagosomes. *Molecular Biology of the Cell.* **15** (12), 5647-58 (2004).

29. Edelstein, A. D., Tsuchida, M. A., Amodaj, N., Pinkard, H., Vale, R. D., Stuurman, N., Advanced methods of microscope control using μManager software. *Journal of Biological Methods.* **1** (2),(2014).

30. Selinummi, J., Seppala, J., Yli-Harja, O., Puhakka, J. A. Software for quantification of labeled bacteria from digital microscope images by automated image analysis. *BioTechniques.* **39** (6), 859-863 (2005).

31. Gui, L., Wereley, S. T. A correlation-based continuous window-shift technique to reduce the peak-locking effect in digital PIV image evaluation. *Experimental Fluids.* **32**, 506-517 (2002).

32. Spatio-temporal analysis of eukaryotic cell motility by improved force cytometry. *Proceedings of the National Academy of Sciences of the United States of America.* **104** (33), 13343-13348 (2007).

33. Hur, S. S., *et al*. Roles of cell confluency and fluid shear in 3-dimensional intracellular forces in endothelial cells. *Proceedings of the National Academy of Sciences of the United States of America.* **109** (28), 11110-11115 (2012).

34. Banerjee, I., *et al.* Cyclic stretch of embryonic cardiomyocytes increases proliferation, growth, and expression while repressing Tgf-β signaling. *Journal of Molecular and Cellular Cardiology.* **79**, 133-144 (2015).

35. Zeldovich, V. B., Robbins, J. R., Kapidzic, M., Lauer, P., Bakardjiev, A. I. Invasive extravillous trophoblasts restrict intracellular growth and spread of *Listeria monocytogenes. PLoS Pathogens.* **7** (3), e1002005 (2011).

36. Wood, J. A., Liliensiek, S. J., Russell, P., Nealey, P. F., Murphy, C. J. Biophysical cueing and vascular endothelial cell behavior. *Materials.* **3** (3), 1620-1639 (2010).

37. Kohn, J. C., Lampi, M. C., Reinhart-King, C. A. Age-related vascular stiffening: causes and consequences. *Frontiers in Genetics.* **6**, 112 (2015).

38. Janmey, P. A., Miller, R. T. Mechanisms of mechanical signaling in development and disease. *Journal of Cell Science.* **124** (1), 9-18 (2011).

39. Wells, R. G. The role of matrix stiffness in regulating cell behavior. *Hepatology.* **47** (4), 1394-1400 (2008).

40. Onken, M. D., Mooren, O. L., Mukherjee, S., Shahan, S. T., Li, J., Cooper, J. A. Endothelial monolayers and transendothelial migration depend on mechanical properties of the substrate. *Cytoskeleton (Hoboken).* **71** (12), 695-706 (2014).

41. Lamason, R. L., *et al*. Rickettsia Sca4 reduces vinculin-mediated intercellular tension to promote spread. *Cell.* **167** (3), 670-683 (2016).

42. Wu, T.-C., Belteton, S., Pack, J., Szymanski, D. B., Umulis, D. LobeFinder: a convex hull-based method for quantitative boundary analyses of lobed plant cells. *Plant Physiology.* **171** (4), 2331-2342 (2016).

43. Czuczman, M. A., *et al.Listeria monocytogenes.* exploits efferocytosis to promote cell-to-cell spread. *Nature.* **509** (7499), 230-234 (2014).

44. Liebhold, A. M., Tobin, P. C. Population ecology of insect invasions and their management. *Annual Reviews in Entomology.* **53**, 387-408 (2008).

45. Miller, C. J., Davidson, L. The interplay between cell signaling and mechanics in developmental processes. *Nature Reviews Genetics.* **14** (10), 733-744 (2013).

46. Mammoto, T., Ingber, D. E. Mechanical control of tissue and organ development. *Development (Cambridge, England).* **137** (9), 1407-1420 (2010).

47. Yeh, Y. T., *et al.* Matrix stiffness regulates endothelial cell proliferation through septin 9. *PLoS One.* **7.** (10), e46889 (2012).

48. Ali, M. Y., Chuang, C. Y., Saif, M. T. Reprogramming cellular phenotype by soft collagen gels. *Soft Matter.* **10** (44), 8829-8837 (2014).

49. Tse, J., Engler, A. Stiffness gradients mimicking *in vivo.* tissue variation regulate mesenchymal stem cell fate. *PLoS ONE.* **6** (1), e15978 (2011).

50. Ananthakrishnan, R., Ehrlicher, A. The forces behind cell movement. *International Journal of Biological Sciences.* **3**, 303-317 (2007).

51. Kolahi, K. S., *et al.* Effect of substrate stiffness on early mouse embryo development. *PLoS ONE.* **7.** (7), e41717 (2012).

52. Caliari, S. R., Burdick, J. A. A practical guide to hydrogels for cell culture. *Nature Methods.* **13** (5), 405-14 (2016).

53. Kiener, H. P., Lee, D. M., Agarwal, S. K., Brenner, M. B. Cadherin-11 induces rheumatoid arthritis fibroblast-like synoviocytes to form lining layers *in vitro. American Journal of Pathology.* **168**, 1486-1499 (2006).

54. Kaliman, S., Jayachandran, C., Rehfeldt, F., Smith, A.-S. Novel growth regime of MDCK II model tissues on soft substrates. *Biophysical Journal.* **106** (7), L25-L28 (2014).

55. Saunders, R. L., Hammer, D. A. Assembly of human umbilical vein endothelial cells on compliant hydrogels. *Cellular and Molecular Bioengineering.* **3** (1), 60-67 (2010).

56. Wu, J., Weening, E. H., Faske, J. B., Hook, M., Skare, J. T. Invasion of eukaryotic cells by *Borrelia burgdorferi.* requires β_1 integrins and Src kinase activity. *Infection and Immunity.* **79** (3), 1338-4138 (2011).

57. Stroka, K. M., Aranda-Espinoza, H. Endothelial cell substrate stiffness influences neutrophil transmigration via myosin light chain kinase-dependent cell contraction. *Blood.* **118** (6), 1632 (2011).

58. Keer, L. M. Stress distribution at the edge of an equilibrium crack. *Journal of the Mechanics and Physics of Solids.* **12** (3), 149-163 (1964).

59. Bastounis, E. E., Theriot, J. A. A highly quantitative multi-well format assay for studying the effect of extracellular matrix mechanics on the bacterial infection of endothelial cells. *Athens Journal of Sciences.* **4** (1), 7-20 (2017).